

A New Spatio-Temporal Equalization Method Based on Estimated Channel Response

The Revised Version 99C200R1

Kazunori Hayashi, *Member, IEEE*, and Shinsuke Hara, *Member, IEEE*

Kazunori Hayashi and Shinsuke Hara are with the Department of Electronic, Information and Energy Engineering, Graduate School of Engineering, Osaka University, Osaka, Japan.

Abstract

This paper proposes a new spatio-temporal equalization method, which simultaneously utilizes an adaptive antenna array and a decision feedback equalizer (DFE). For effective spatio-temporal equalization with less computational cost, how to split equalization functionality into spatial processing and temporal processing is quite important. One of the answers which we have given is ‘incoming signals with larger time delays should be cancelled at the spatial equalization part.’ The weights of both adaptive antenna array elements and taps of DFE are calculated only using estimated channel impulse response, therefore, it requires no information on direction of arrival (DoA). We show the performance of the proposed system in multipath fading channels often encountered in indoor wireless environments, and discuss the attainable bit error rate (BER), antenna patterns, and the computational complexity in comparison with other equalization methods, such as spatial equalization and temporal equalization.

Index Terms- wireless LAN, Adaptive arrays, Array signal processing, Decision feedback equalizers, equalization

I. INTRODUCTION

Space resource has been drawing much attention as an essential orthogonal resource in fourth generation wireless communications systems. It is because space orthogonality provides virtual wired communication which is suited to support multimedia services. At present, space resource is not made good use of in wireless communications systems, therefore, its efficient use has a dramatic potential to break through the system performance. This is the reason why now spatial and temporal signal processing is a hot topic of research[1], [2].

Spatio-temporal equalization is a technique which utilizes both spatial and temporal information of received signal to compensate intersymbol interference due to multipath fading. So far, a considerable number of studies have been made on spatio-temporal equalization, and a lot of the equalization methods have been proposed[3]-[6]. However, though the equalization methods can achieve good performance, they require high computational complexity. This is because almost all the methods employ an adaptive antenna array which has temporal filter at each antenna element (i.e. broadband beamformer[7]) or maximum likelihood sequence estimation (MLSE) approach in weights calculation. In this paper, attaching greater importance to computational complexity, we consider a configuration of spatio-temporal equalizer with less computational cost, such that *an adaptive antenna array without temporal filter* is followed by a decision feedback equalizer (DFE).

What is important to realize effective spatio-temporal equalization with such a configuration is how to split equalization functionality into spatial processing and temporal processing. In this paper, we take a fundamental strategy based on ‘*incoming signals with larger time delays should be cancelled at the spatial equalization part.*’ This is because the performance of spatial equalizer does not depend on the time delay, on the other hand, the computational complexity of temporal processing largely depends on the maximum length of the time delay. The proposed configuration itself is similar to that of the conventional method proposed in [8], where a diversity system and a DFE are smartly combined. However, the conventional method requires that received signals on different antenna elements are statistically independent, because the antenna array in the conventional system is based on a diversity system. On the other hand, the spatial equalizer in our system is based on a beamformer, therefore, the proposed system can achieve good performance regardless of correlation among the received signals.

Array signal processing contains many applications such as direction of arrival (DoA) estimation and beamforming, and there are a lot of algorithms for them. Such algorithms can be applied to the spatial equalizer, however, it becomes a problem that the determination of the weights of adaptive antenna array elements could require both DoA estimation and beamforming procedures, in other words, the spatial equalization could be made in two steps, with different characteristics of processing. In order to avoid the two-step approach, we have been proposing a spatial equalization method [9], where the beamformer calculates and adjusts the weights of adaptive array elements only using an estimated channel impulse response, and we have clearly shown that the weights of adaptive antenna array elements can be successfully controlled by the estimated channel impulse response and that the proposed beamformer can achieve better bit error rate (BER) performance than a constant modulus algorithm (CMA)[10] based beamformer. Here, taking into account that the estimated channel impulse response can be also used for the temporal equalization part, it is quite natural that we can easily extend the idea of ‘impulse response estimation-based control’ in the spatial equalization to a basic strategy in spatio-temporal equalization.

There are basically two different kinds of strategies for channel impulse response estimation, such as blind approach and pilot-assisted approach. Blind estimation can achieve high transmission efficiency because of no pilot signal transmission. However it still has a problem of late convergence,

though a lot of fast and accurate methods just using second-order statistics have been proposed[11]-[13]. For pilot-assisted approach, transmitter classically inserts known pilot signal at the top end of signal frame, and at receiver end, equalizer adjusts its weights every frame timing. In such a system, the weight calculation time must be shorter than a period of one frame, otherwise, it is impossible to process. However, even in high speed wireless communications using short length frame, such as wireless asynchronous transfer mode (ATM), variation speed of fading does not depend on data transmission speed and hence it is not necessary to update the weights for each frame timing, or rather say, it is sufficient to update the weights slowly enough to follow the fading. Therefore, in the proposed system, the pilot signal, which consists of pseudo noise (PN) sequence and has the same bandwidth as the data signal, is superimposed on the data signal with the power suppressed enough. Though the pilot signal and data signal are not orthogonal in frequency and time domains, we can extract the pilot signal by correlation (despreading). The usage of such a suppressed pilot signal brings about some attractive features. The main advantage is that we can independently handle the data demodulation process and the spatial/temporal control process. This means that we can separate the weight calculation, which often requires high computational complexity, from the data signal processing, therefore, high speed demodulation processing can be achieved. It will be also the reason why the proposed scheme is suited for high speed communications that all the time slots can be used for user data. In addition, since the weights are calculated from the estimated channel response, there is no limitation in the modulation format of the data signal. However, on the other hand, the proposed system has a disadvantage that the pilot signal gives interference to the data signal. Therefore, to suppress the power enough, keeping good estimation and equalization performance, is also a key issue in the paper. In order to annihilate interference from pilot signal, a Code Division Multiple Access (CDMA)-like technique could be applicable, where orthogonal spreading codes are assigned to both the pilot and data signals[14]. However, in order to achieve high data transmission speed, a lot of spreading codes need to be assigned to one user (multiple codes assignment in CDMA system), so it could result in fluctuations of the transmitted signal and increase of complexity in transmitter and receiver structures.

In this paper, we discuss a new spatio-temporal equalization method only employing channel impulse response estimation. We show the BER performance for the proposed spatio-temporal equalizer in multipath fading channels often encountered in indoor wireless environments. We also compare the performance among a temporal equalizer (DFE), a spatial equalizer (our already-proposed beamformer), and the proposed spatio-temporal equalizer. Moreover, we evaluate the computational complexity required in the spatio-temporal processing.

This paper is organized as follows: Section 2, 3 and 4 describe the system configuration, the pilot signal extraction and the beamforming method, respectively. Numerical results are presented in Section 5. Finally, conclusions are given in Section 6.

II. SYSTEM CONFIGURATION

Assume that the proposed spatio-temporal equalizer is applied to the down link of a wireless local area network (LAN) system, where a base station with an omnidirectional antenna communicates with n terminals each having an adaptive antenna array and a DFE. Fig.1 shows the transmitter/receiver structure. In our method, we prepare two types of channels; a traffic channel and a pilot channel. The traffic channel is used to convey information signals, and the pilot channel to estimate channel impulse response for weights (of both spatial and temporal equalizers) calculation.

In the transmitter, data sequence (R_b [bits/sec]) is first converted into QPSK waveform ($R_s (=R_b/2)$ [symbols/sec]) for the traffic channel, on the other hand, known pilot signal is generated by the PN sequence generator for the pilot channel, which has the same frequency band width as the traffic channel. Note that PN sequence generators generate two different PN sequences, which are respectively used for inphase and quadrature pilot channels (I and Q-ch) after QPSK modulation. In addition, the power of the pilot signal is suppressed enough before the addition to the data signal. If we use a S_{pn} -stage maximum length shift register (M-) sequence as a PN sequence, the period of the PN sequence becomes P ($= 2^{S_{pn}} - 1$) symbols long.

Let $s_B(t)$, $s_{Tr}(t)$, and $s_{Pi}(t)$ denote the baseband transmitted signal, the data signal, and the pilot signal, respectively. They can be written as

$$s_B(t) = s_{Tr}(t) + \sqrt{\beta} \cdot s_{Pi}(t), \quad (1)$$

$$s_{Tr}(t) = \sum_{k=-\infty}^{\infty} d_k \delta(t - kT_s), \quad (2)$$

$$s_{Pi}(t) = \sum_{l=-\infty}^{\infty} \sum_{k=0}^{P-1} m_k \delta(t - (lP + k)T_s), \quad (3)$$

$$d_k = d_{I_k} + jd_{Q_k}, \quad (4)$$

$$m_k = m_{I_k} + jm_{Q_k}, \quad (5)$$

where d_{I_k} and d_{Q_k} denote the k th symbol of the inphase and quadrature components in the data signal, respectively. T_s , β , and $\delta(y)$ denote the time duration of one symbol, the power suppression ratio of the pilot channel, and the Dirac's delta function, respectively. Moreover, m_{I_k} and m_{Q_k} express the inphase and quadrature components of the pilot signal at the k th symbol, respectively.

The baseband signal passes through the low pass filter (LPF), i.e., emission filter, and then is transmitted from the omnidirectional antenna after up-conversion. The transmitted signal $s_T(t)$ will be

$$s_T(t) = \text{Re}[z_0(t) \exp(j2\pi f_c t)], \quad (6)$$

$$z_0(t) = s_B(t) * h_B(t), \quad (7)$$

where $h_B(t)$, f_c , and $z_0(t)$ denote the impulse response of the LPF, the carrier frequency, and the band-limited baseband signal, respectively.

In the receiver, the incoming signal is received by the antenna array which consists of N_{ary} sensors, where the sensor spacing is the half of carrier wavelength. After then, the received signal undergoes the band pass filter (BPF), down-converter, LPF (matched filter), and A/D converter. The BPF is used for the suppression of the adjacent channel interference and noise as well as for the extraction of the spectrum around the desired signal. Moreover, the A/D converter operates with the sampling rate of N_{samp} times the symbol rate. After the A/D conversion, the received signal is processed in the traffic channel processing part and in the weight calculation part independently.

In the traffic channel processing part, the outputs from the matched filters are multiplied by the weights of the beamformer which are calculated in the weight calculation part. After symbol timing synchronization and equalization with DFE which has N_{ftap} taps in the feedforward filter and N_{btap} taps in the feedback filter, the data are recovered.

In the weight calculation part, the complex instantaneous channel impulse response at each antenna element is first estimated by correlating the received pilot signal. The estimated channel impulse response is used to calculate the impulse response for the reference signal generation.

Details of the reference signal generation are discussed in Section 4. Next, a QPSK signal is generated in the receiver and is fed into the filter whose tap coefficients are the same as the estimated channel impulse response, and as a result, the output of the filter becomes a pseudo-received pilot signal (without data signal). Note that, in our approach, the pilot signal is sent as a PN code which is superposed on the data signal, therefore, the received pilot signal itself can not be obtained as a training signal for weight calculation.

On the other hand, the generated QPSK signal is also fed into the filter whose tap weights are the same as the impulse response for the reference signal generation. Using the output of this filter as a reference signal and the pseudo-received pilot signal, the weights of antenna elements are calculated by the recursive least square (RLS) algorithm[16].

Now that the estimated channel impulse response and the weights of the adaptive antenna array elements are available, we can calculate the tap weights of the DFE by the RLS algorithm in the same manner as the beam-weights calculation.

Finally, we summarize the flow of signal processing in the receiver (see Fig.2). In the figure, the hatched procedures show a series of signal processing: the receiver first extracts pilot signals from received signals and then estimates the channel impulse response using the signals. During the next frame, the receiver calculates the weights of the beamformer and the DFE (see Fig.2 a). Further, at the end of the frame, the weights are updated and then are used for the processing of the traffic channel (see Fig.2 b).

III. PILOT SIGNAL EXTRACTION

Fig.3 shows the signal frame structure of the proposed system. The length of one frame is P (the period of the PN sequence in the pilot channel) times N_{pnseq} symbols. The complex instantaneous channel impulse response is calculated using the received pilot signals of the frame.

The received signals first pass through the matched filter for the pilot channel. By means of this procedure, N_{pnseq} complex instantaneous impulse responses without sufficiently suppressed traffic channel are obtained. And then, by coherently adding these, the impulse response with sufficiently suppressed traffic channel is generated.

The processing gain of the pilot channel G_p becomes

$$G_p = P \times N_{pnseq}, \quad (8)$$

and since the power ratio of the pilot channel to the traffic channel is equal to β , the power ratio between the pilot channel and the traffic channel at the time of calculating the complex channel impulse response is given by

$$G_{total} = G_p \beta = P \times N_{pnseq} \beta. \quad (9)$$

IV. BEAMFORMING METHOD

In the weight calculation part, we first estimate the channel impulse response. Let $g_l(t)$ denote the output of the matched filter at the l th antenna element. In the proposed system, since the observation window width of the channel impulse response is equal to P symbols, the estimated channel impulse response at the k th estimation window can be written as

$$\hat{h}_l^k(\tau) = \sum_{i=0}^{N_{smp} \times P - 1} g_l(t_k + i \frac{T_s}{N_{smp}}) \delta(\tau - i \frac{T_s}{N_{smp}}), \quad (0 \leq \tau \leq P \times T_s) \quad (10)$$

where $\hat{(\cdot)}$ denotes the estimation of (\cdot) .

Fig.4 shows an example of the estimated impulse response. As we mentioned in Section 3., the channel impulse response is estimated using $P \times N_{pnseq}$ received pilot signals, therefore, the estimated channel impulse response at the l th antenna element \hat{h}_l will be obtained by averaging out $\hat{h}_l^k(\tau)$, namely,

$$\hat{h}_l(\tau) = \frac{1}{N_{pnseq}} \sum_{k=1}^{N_{pnseq}} \hat{h}_l^k(\tau). \quad (11)$$

Next, we search for a path with the maximum power. In other words, defining

$$\sigma(\tau) = \sum_{l=1}^{N_{ary}} |\hat{h}_l(\tau)|^2, \quad (12)$$

as the total power at τ , we search for $\tau = \tau_{max}$ such that $\sigma(\tau)$ is maximal. Using τ_{max} , we can estimate the channel impulse response at the l th antenna element including the path with the maximum power as

$$f_l(k) = \hat{h}_l(\tau_{max} + kT), \quad (1 \leq l \leq N_{ary}), \quad (13)$$

which has a non-zero value for k satisfying $0 \leq \tau_{max} + kT_s \leq P \times T_s$ and zeros otherwise.

The impulse response $f_l(k)$ is used to generate the pseudo-received pilot signal at the l th antenna element $x'_l(k)$:

$$x'_l(k) = d'(k) * f_l(k) + n'_l(k), \quad (14)$$

where $*$ denotes the convolution, $d'(k)$ is the QPSK (pilot) signal generated in the receiver, and $n'_l(k)$ is also the generated white Gaussian noise, whose power is equal to that of the noise in the channel. Since the noise has all kinds of phase components and hence all DoA components, the excess beam which only captures the noise can be suppressed by the addition of the noise. The important point to note is that the proposed system requires not the accurate knowledge on noise power but the spatial whiteness of the noise for the noise suppression. This is because, unlike in the case of temporal filters, adaptive array can eliminate the delayed signals without giving large gain to any spatial frequency components. Thus, the elimination of the delayed signals and the suppression of the noise have no trade-off relationship. As a result, the performance of the proposed system is not sensitive to the noise power in the pseudo-received pilot signal, and we can fix the ratio of the energy per symbol to the noise power density (E_s/N_0) of the pseudo-received pilot signal, for instance, 20dB, in advance.

The impulse response for the reference signal generation is generated from the N_{ary} estimated channel responses. From a statistical point of view, there is no difference among the estimated channel responses, therefore, the response at the 1st antenna element is employed as the response for the reference generation. However, considering the effect of fading, the amplitude is chosen to be the average of the estimated responses among the antenna elements. In the end, the impulse response for the reference signal generation $f_{ref}(k)$ can be written as

$$f_{ref}(k) = \frac{1}{N_{ary}} \left(\sum_{l=1}^{N_{ary}} |f_l(k)| \right) \frac{f_1(k)}{|f_1(k)|}, \quad (15)$$

$$(0 \leq k \leq N_{feedback})$$

where $N_{feedback}$ denotes the length of the feedback filter in the DFE, and $f_{ref}(k)$ is equal to zero for $k > N_{feedback}$. In the proposed system, the incoming signal whose delay time exceeds the length of feedback filter in the DFE is canceled at the spatial equalization part.

The reference signal $x'_{ref}(k)$ can be written as

$$x'_{ref}(k) = d'(k) * f_{ref}(k), \quad (16)$$

and finally, with this reference signal $x'_{ref}(k)$ and the pseudo-received pilot signal $x'_l(k)$, the weights of beamformer are calculated by the RLS algorithm.

V. COMPUTER SIMULATION

A. Channel Model

Computer simulations are conducted to evaluate the performance of the proposed spatio-temporal equalizer in comparison with a temporal equalizer (DFE[15]), and a spatial equalizer (our already-proposed beamformer[9]). Parameters used in all the computer simulations are summarized in Table I. Considering indoor wireless environments, DoAs of incoming signals will be distributed from $-\pi$ to π . Therefore, we adopted not a linear array, whose beamforming ability significantly degrades for a particular direction, i.e., parallel to the linear array, but a circular array (with 4 elements), which can achieve almost uniform beamforming performance for all directions. The proposed system also employs a DFE which has 9taps (5taps in the feedforward filter and 4taps in the feedback filter).

The number of repetitions of the RLS algorithm in both the spatial equalization part N_{cal_S} and the temporal equalization part N_{cal_T} are chosen to be 50. In the spatial equalizer, the same antenna array as the proposed system is employed, while the equalizer has no temporal equalization part. The number of repetitions of the RLS algorithm N_{cal_S} is also the same as the proposed system. On the other hand, the temporal equalizer employs an omnidirectional antenna and a DFE which has 19taps (10taps in the feedforward filter and 9taps in the feedback filter). The same number of repetitions of the RLS algorithm N_{cal_T} is also employed. Since the temporal equalizer employs an omnidirectional antenna, and the spatial and the proposed equalizer have four antenna elements, in the following figures, the curves of the BER performance of the temporal equalizer will be shifted by 6dB. In all the systems, we adopt a root Nyquist filter with roll-off factor α of 0.5 as the LPF in the transmitter and receiver. Also, we adopt the symbol rate R_s of 100[Msymbols/sec], the oversampling factor N_{smp} of 4, the period of M-sequence P of 255[symbols], and the carrier frequency f_c of 60[GHz]. Taking account of an indoor environment, we set the Doppler shift to 150[Hz].

Fig.6 shows the frequency selective fading channel model used for the optimization of parameters. There are 4 preceding signals and 2 four-symbol delayed signals, where the power ratio of these 6 incoming signals are the same.

Fig.7 also shows the frequency selective fading channel model discussed, where there are 5 preceding signals and 5 one-symbol delayed signals. The power ratio of these 10 incoming signals are also the same. DoA of each incoming signal is randomly determined and it changes every frame timing.

Fig.8 shows the static 3-ray multipath channel model. There is a preceding signal in the same direction as a two-symbol delayed signal, and there is one more incoming signal which has a large (eight-symbol) delay time. We discuss the attained performance based on the channel model B among a temporal equalizer, the spatial equalizer, and the proposed spatio-temporal equalizer.

When the BER characteristics are evaluated, it is considered effective to compare the results with the theoretical BER of diversity reception, or to confirm how many branches as diversity gain the results correspond to. Assuming the average power of each signal is the same and the

envelope follows a Rayleigh distribution, the BER of QPSK in the case of the L branch maximum ratio combining diversity is given[15],

$$BER = \left(\frac{1-\mu}{2}\right)^L \sum_{k=0}^{L-1} C_k \left(\frac{1+\mu}{2}\right)^k, \quad (17)$$

$$\mu = \sqrt{\frac{\overline{\gamma}_s/2}{1 + \overline{\gamma}_s/2}}, \quad (18)$$

where $\overline{\gamma}_s$ is E_s/N_0 . On the other hand, the BER in an additive white Gaussian noise (AWGN) channel is given by the following[15],

$$BER = \frac{1}{2} \operatorname{erfc}\left(\sqrt{N_{ary} \cdot \gamma_s/2}\right), \quad (19)$$

where $\operatorname{erfc}(\cdot)$ is the complementary error function. Note that γ_s is multiplied by the number of sensor.

B. Parameter Setting

Since the data signal and the pilot signal in the proposed system are not orthogonal, in other words, the pilot signal can be considered to be a co-channel interference, the performance depends on the power suppression ratio β of the pilot channel and the number of coherent additions N_{pnseq} after correlating. Thus, we discuss these values first. In the proposed system, it is found from Eq.(9) that if β or N_{pnseq} increases, the measurement accuracy of the channel impulse response is improved. However, it is more efficient to make β smaller and N_{pnseq} larger from the viewpoint of power efficiency, whereas it is preferable to make β larger and N_{pnseq} smaller from the viewpoint of tracking of fading variations. Therefore, it is considered that there is an optimum point in β and N_{pnseq} to maximize the performance.

Fig.9 shows the BER versus β and G_{total} for several values of N_{pnseq} , when we assume the channel model A with $\overline{E_s/N_0}=16\text{dB}$, where $\overline{(\cdot)}$ denotes the average of (\cdot) . Here, note that E_s includes both the user signal and the pilot signal unlike the theoretical equation (Eqs.(17)-(19)). Hereafter, we use this new definition of E_s . The performance is poor for large β , because the power assigned to the traffic channel becomes smaller, whereas the BER degrades for smaller β , because the measurement accuracy of the channel impulse response becomes poor. From this figure, we selected $N_{pnseq}=16$ and $\beta=0.04$ as the optimum values, which correspond to $G_p=4,080$ and $G_{total}=163.2$.

C. Bit Error Rate Performance

Fig.10 shows the BER versus E_s/N_0 in an AWGN channel. We can recognize about 2dB degradation from the theoretical line. This may be because of the insertion of the pilot channel, and the error in the channel impulse response estimation or in the spatial and temporal weights calculation. The effect of the four times over sampling also may be the cause of the degradation. However, as we can see from Fig.9, both of the first two degradation sources, i.e., the insertion of the pilot channel and the error in the channel identification, severely affect the BER performance. Also, the two degradation sources have a trade-off relationship. Since we have optimized the power of the pilot signal so as to maximize the performance, the influence caused by the two sources will be almost the same degree.

Fig.11 shows the BER performance in the channel model B. The BER performance of the spatial equalizer (our already-proposed beamformer) and the temporal equalizer is also plotted in the same figure. The BER of the temporal equalizer improves gradually as $\overline{E_s/N_0}$ increases, but the performance is the worst among the three equalizers. The spatial equalizer can achieve the fairly good performance, however, we can recognize the BER floor for $\overline{E_s/N_0} > 15\text{dB}$. Since DoAs in this channel model are randomly determined every frame timing, the spatial equalizer sometimes can not equalize the distorted received signal. Namely, the burst errors occur in certain DoA patterns. This is the reason for the BER floor. On the other hand, the proposed system can achieve the best performance among the three equalizers and the gain of 3-branch maximal-ratio combining diversity. In addition, no error floor can be recognized. This means that the burst errors, which have been observed in the spatial equalizer case, do not occur in any DoA patterns. It can be concluded, therefore, the equalization of the proposed system does not care DoA patterns.

Fig.12 shows the BER performance in the channel model C. The performance of the spatial equalizer is the worst among the three equalizers. The spatial equalizer forms its beam as capturing the path with the maximum power, therefore, it tries to catch the *signal a*. However, since the *signal a* is in the same direction as the delayed signal (*signal b*), the received signal suffers from intersymbol interference. This is the reason for the poor performance of the spatial equalizer. The performance of the temporal equalizer also improves gradually as E_s/N_0 increases in this channel model. However, the proposed system can achieve much better performance. In this channel model, the proposed system cancels the *signal c*, which has large time delay, at the spatial equalization part. Accordingly, all the temporal equalization part has to do is to cancel the *signal b*.

D. Antenna Patterns

Here, the difference in operation between the proposed spatio-temporal equalizer and the spatial equalizer is analyzed from the antenna patterns. Figs.13, 14 and 15 show the antenna patterns. In all the figures, the primary signal and the 1- and 8-symbol delayed signals are arriving, and the power ratio of these 3 signals is 2 : 1 : 1.

In Fig.13, the primary signal is arriving from the direction of 18[deg] and the 1- and 8-symbol delayed signals are arriving from the direction of 72 and 270[deg], respectively. In this case, both of the equalizers are likely to work well, however, the BER of the proposed equalizer is worse than that of the spatial equalizer. This is mainly because the proposed equalizer gives smaller gain for the primary signal than the spatial equalizer does.

In Fig.14, the primary signal and the 1-symbol delayed signal are arriving from the direction of 18[deg], and the 8-symbol delayed signal is arriving from the direction of 299[deg] (This is the same channel model as the channel model C(Fig.8)). As described above, the spatial equalizer controls the beam in the direction of 18[deg], therefore, the BER is poor. However, the proposed system controls the null in the direction of 299[deg], and equalizes the primary signal which is collapsed only by the 1-symbol delayed signal at the temporal equalization part.

In Fig.15, the primary signal and the 1- and 8-symbol delayed signals are arriving from the direction of 45, 225 and 299[deg], respectively. The primary signal and the delayed signals are not in the same or near direction, therefore, it is expected that the BER of the spatial equalizing method will be good. However, in practice, the spatial equalizer can not extract only the primary signal and the error rate is poor. This is a matter of the limitation of the degrees of freedom in forming beams. Adaptive antenna array can form various beampatterns, however, this does not

mean that it can make arbitrary beampattern. Namely, if a beam is controlled in one direction, it may results in forming another beam toward another direction. Setting coordinate as in Fig.16, the beampattern $R(\theta)$ can be written as

$$R(\theta) = \left| \sum_{l=1}^{N_{ary}} \exp[j\cos(\frac{\pi}{2}l - \theta)]w_l \right|^2, \quad (20)$$

where w_l denotes the weight corresponding to the l th antenna element. From Eq.(20), it turns out that the antenna array can not have such a beampattern that $R(\pi/4) = 1$ and $R(5\pi/4) = 0$. Therefore, the weights of the spatial equalizer do not converge well. This is the reason of the poor BER performance of the spatial equalizer. However, the proposed system works properly, that is, the delayed signal with large time delay is cancelled at the spatial equalization part.

E. Computational Cost

We show the number of multiplications in the weights calculation algorithm as a computational cost. In the following, N_{tap} denotes the total number of taps in the DFE, namely, $N_{tap} = N_{ftap} + N_{btap}$. For the proposed system, the number of multiplication in the weight calculation algorithm is

$$\begin{aligned} & N_{cal_S} \times (16N_{ary}^2 + 18N_{ary} + 1) \\ & + N_{cal_T} \times (16N_{tap}^2 + 18N_{tap} + 1) \\ & = 89,400 \text{ (times)}, \end{aligned}$$

for the spatial equalizer,

$$\begin{aligned} & N_{cal_S} \times (16N_{ary}^2 + 18N_{ary} + 1) \\ & = 16,450 \text{ (times)}, \end{aligned}$$

and for the temporal equalizer (DFE),

$$\begin{aligned} & N_{cal_T} \times (16N_{tap}^2 + 18N_{tap} + 1) \\ & = 305,950 \text{ (times)}. \end{aligned}$$

The spatial equalizer requires the least computational complexity, but it suffers from break down of the equalization for certain DoA patterns. The computational complexity of the temporal equalizer depends on the maximum time delay of the incoming signal which we must equalize. Therefore, the temporal equalizer may be not suited for high speed communications. The proposed spatio-temporal equalizer not only can achieve an excellent BER performance but also requires a relatively low computational cost.

VI. CONCLUSIONS AND DISCUSSIONS

In this paper, we have proposed a new spatio-temporal equalization method and evaluated its performance comparing with a spatial equalizer and a temporal equalizer. Here, our fundamental criterion is ‘delayed incoming signals with large time delays should be canceled by the spatial equalization part’, which makes it possible to decrease the computational complexity. It goes without saying that if we only consider the performance, our criterion can not be true in general. However, if we regard the computational complexity as important, our criterion could be a good

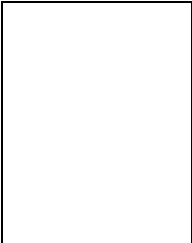
choice. In addition, the proposed equalizer only uses estimated channel impulse response to adjust the weights of the beamformer and the DFE, therefore, it requires no information on DoA.

We have shown the attainable BER performance in an AWGN channel, a frequency selective fading channel, and a static 3-ray multipath channel. Moreover, we have analyzed the operation of the spatial equalization part of the proposed system from a viewpoint of antenna patterns. We have also shown the computational complexity in terms of the number of multiplications in the total weight calculation. From all the results, it can be concluded that the proposed system can achieve the best and stable performance among the three equalization methods with a relatively low computational complexity.

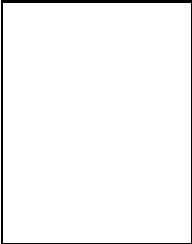
Many blind channel identification algorithms are now available[11]-[13], therefore, the proposed spatio-temporal equalization method may be able to be developed to work in a blind manner by employing such algorithms. The investigation of the proposed system combining the blind channel identification is in progress.

REFERENCES

- [1] R. Kohno, "Spatial and Temporal Communication Theory Using Adaptive Antenna Array," *IEEE Personal Communications*, pp.28-35, Feb. 1998.
- [2] A. J. Paulraj and B. C. Ng, "Space-Time Modems for Wireless Personal Communications," *IEEE Personal Communications*, pp.36-49, Feb. 1998.
- [3] G. E. Bottomley and K. Jamal, "Adaptive Arrays and MLSE Equalization," *Proc. VTC*, vol. 1, pp.50-54, July 1995.
- [4] S. N. Diggavi and A. Paulraj, "Performance of Multisensor Adaptive MLSE in Fading Channels," *Proc. VTC*, vol. 3, pp.2148-52, May 1997.
- [5] Y. Doi, T. Ohgane, and E. Ogawa, "ISI and CCI Canceller Combining the Adaptive Array Antennas and the Viterbi Equalizer in a Digital Mobile Radio," *Proc. VTC*, pp.81-85, Apr. 1996.
- [6] B. C. Ng, J. T. Chen, and A. Paulraj, "Space-Time Processing for Fast Fading Channels with Co-Channel Interference," *Proc. VTC*, pp.1491-95, Apr. 1996.
- [7] B. D. Van Veen and K. M. Buckley, "Beamforming: A Versatile Approach to Spatial Filtering," *IEEE ASSP Magazine*, pp.4-24, Apr. 1988.
- [8] P. Balaban, and J. Salz, "Dual Diversity Combining and Equalization in Digital Cellular Mobile Radio," *IEEE Trans. Veh. Technol.*, vol. 40, no. 2, pp.342-354, May. 1991.
- [9] K. Hayashi, N. Murashima, S. Hara, S. Sampei, and N. Morinaga, "A Beamforming Method Using Suppressed Pilot Signal," *IEICE Trans. Commun.*, Vol.J81-B-I No.11, pp661-70, Nov. 1998.
- [10] J. R. Treichler and B. G. Agee, "A New Approach to Multipath Correction of Constant Modulus Signals," *IEEE Trans. Acoust., Speech, and Signal Processing*, vol.ASSP-31, pp. 459-72, Apr. 1983.
- [11] E. Moulines, P. Duhamel, J. F. Cardoso, S. Mayargue, "Subspace Methods for the Blind Identification of Multichannel FIR Filters," *IEEE Trans. Signal Processing*, Vol. 43, No. 2, pp. 516-25, Feb. 1995.
- [12] G. Xu, H. Liu, L. Tong, T. Kailath, "A Least-Square Approach to Blind Channel Identification," *IEEE Trans. Signal Processing*, Vol. 43, No. 12, pp. 2982-93, Dec. 1995.
- [13] L. Tong, and S. Perreau, "Multichannel Blind Identification: from Subspace to Maximum Likelihood Method," *Proc. IEEE*, Vol. 86, No. 10, pp 1951-68, Oct. 1998.
- [14] E. H. Dinan and B. Jabbari, "Spreading Codes for Direct Sequence CDMA and Wideband CDMA Cellular Networks," *IEEE Comm. Magazine*, pp. 48-54, Sept. 1998.
- [15] J. G. Proakis, *Digital Communications*, Third Edition, McGraw-Hill, 1995.
- [16] S. Haykin, *Adaptive Filter Theory*, Third Edition, Prentice Hall, 1996.



Kazunori Hayashi (S'99) received the B.Eng. and M.Eng. degrees in communication engineering from Osaka University, Osaka, Japan, in 1997 and 1999, respectively. He is currently a Ph.D. candidate at Graduate school of Engineering, Osaka University. His research interests include digital signal processing. He is a student member of IEICE of Japan.



Shinsuke Hara (S'87-M'90) received the B.Eng., M.Eng. and Ph.D. degrees in communication engineering from Osaka University, Osaka, Japan, in 1985, 1987 and 1990, respectively. From April 1990 to March 1996, he was an Assistant Professor in the Department of Communication Engineering, Osaka University. Since April 1996, he has been with the Department of Electronic, Information and Energy Engineering, Graduate School of Engineering, Osaka University, and now, he is an Associate Professor. Also from April 1995 to March 1996, he was a Visiting Scientist at Telecommunications and Traffic Control Systems Group, Delft University of Technology, Delft, The Netherlands. His research interests include satellite, mobile and indoor wireless communications systems, and digital signal processing.

LIST OF TABLES

| | | |
|---|----------------------|----|
| I | Parameters | 14 |
|---|----------------------|----|

LIST OF FIGURES

| | | |
|----|--|----|
| 1 | Transmitter/Receiver Structure | 15 |
| 2 | Flow of Signal Processing | 16 |
| 3 | Pilot Signal Extraction | 16 |
| 4 | Estimated Instantaneous Impulse Response | 17 |
| 5 | Reference Impulse Response | 17 |
| 6 | Channel Model A (frequency selective fading channel) | 17 |
| 7 | Channel Model B (frequency selective fading channel) | 18 |
| 8 | Channel Model C (static 3-ray multipath channel) | 18 |
| 9 | Bit Error Rate versus β and G_{total} | 19 |
| 10 | Bit Error Rate Performance in AWGN Channel | 19 |
| 11 | Bit Error Rate Performance in Channel Model B | 20 |
| 12 | Bit Error Rate Performance in Channel Model C | 20 |
| 13 | Antenna Pattern a | 20 |
| 14 | Antenna Pattern b | 21 |
| 15 | Antenna Pattern c | 21 |
| 16 | Antenna Arrangement | 21 |

TABLE I
PARAMETERS

| | proposed | spatial | temporal |
|---|-------------------|---------|----------|
| Number of sensors N_{ary} | 4 | 4 | 1 |
| Number of feedforward taps N_{ftap} | 5 | - | 10 |
| Number of feedback taps N_{btap} | 4 | - | 9 |
| Symbol rate R_s | 100[Msymbols/sec] | | |
| Oversampling factor N_{smp} | 4 | | |
| Carrier frequency f_c | 60[GHz] | | |
| Roll-off factor α | 0.5 | | |
| Period of the M-sequence P | 255[symbols] | | |
| Repetitions of the RLS algorithm N_{cal_S}, N_{cal_T} | 50 | | |

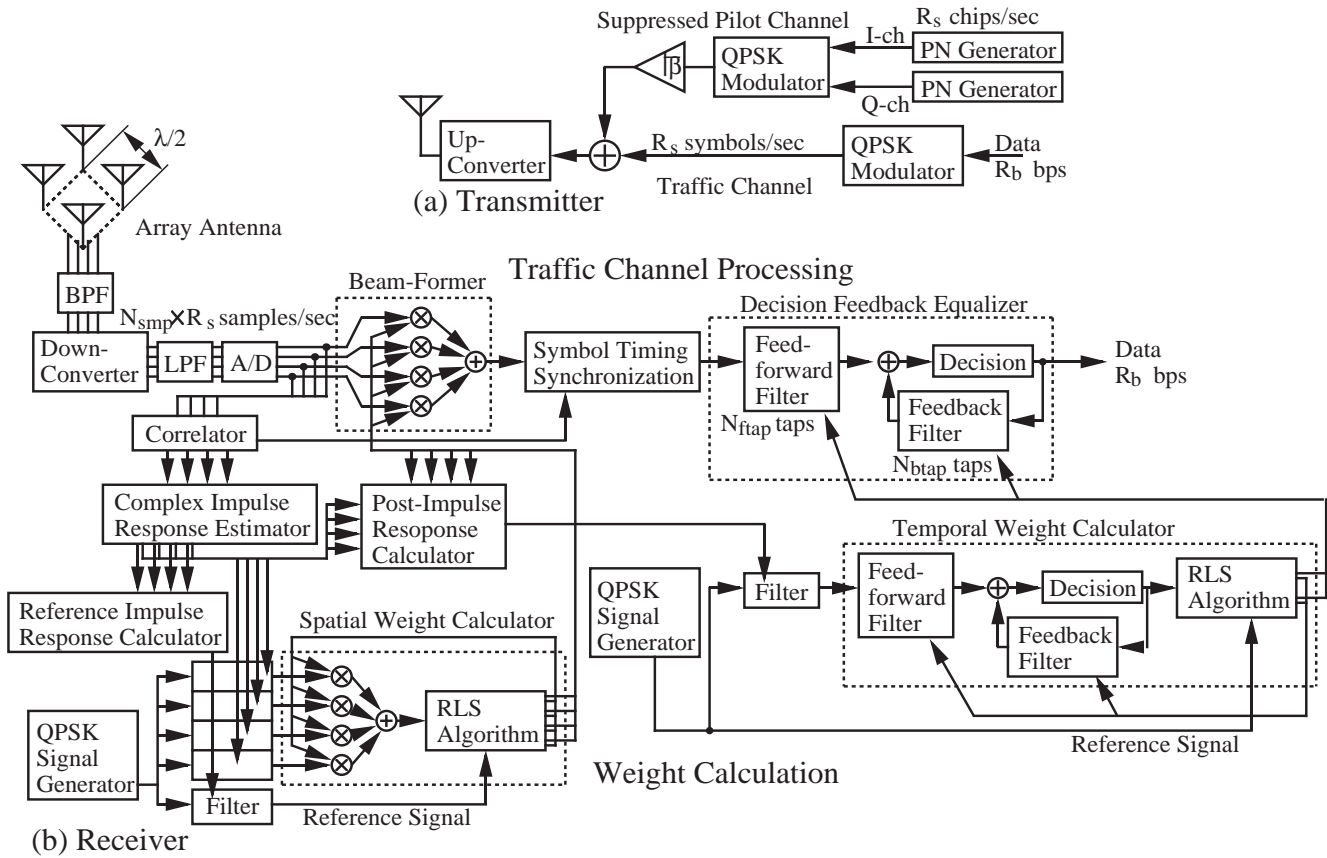


Fig. 1. Transmitter/Receiver Structure

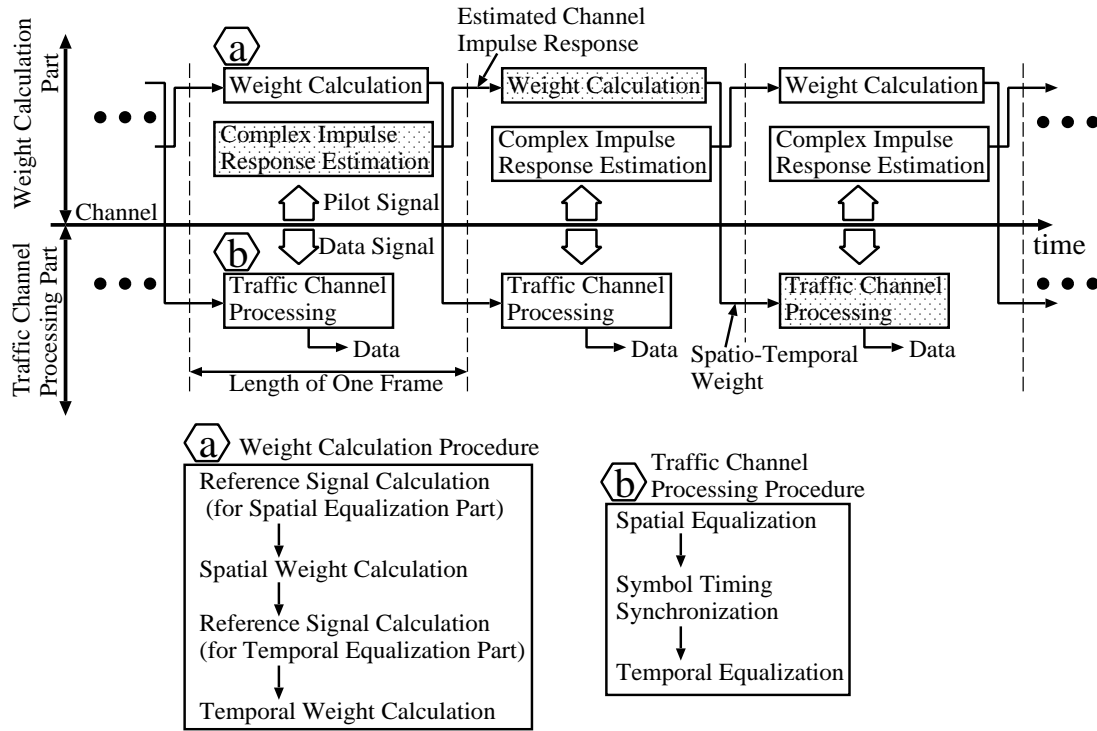


Fig. 2. Flow of Signal Processing

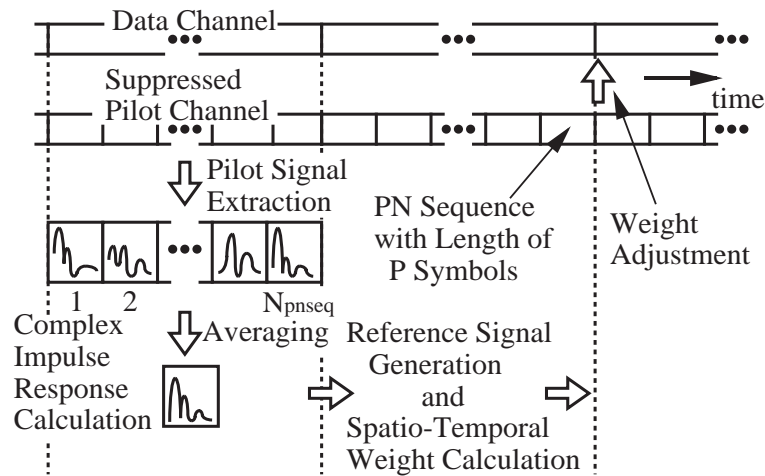


Fig. 3. Pilot Signal Extraction

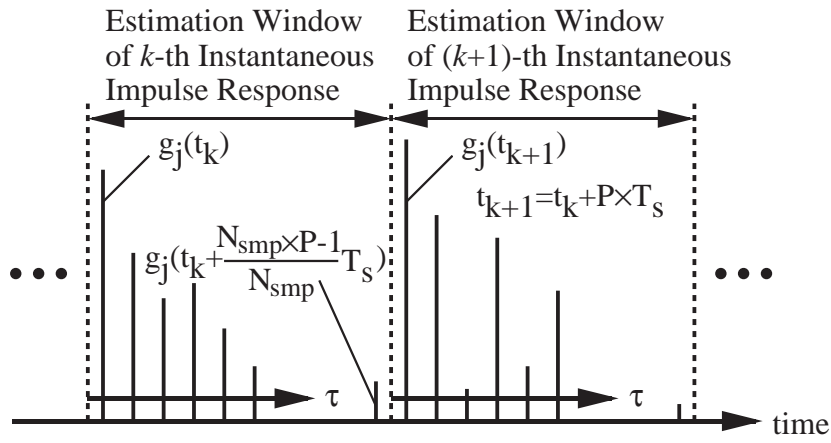


Fig. 4. Estimated Instantaneous Impulse Response

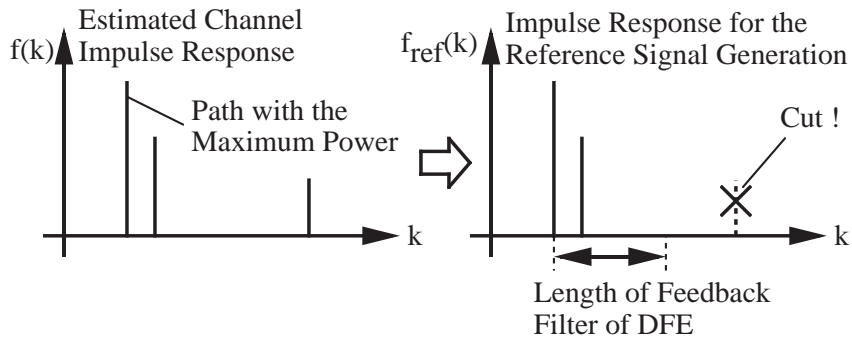


Fig. 5. Reference Impulse Response

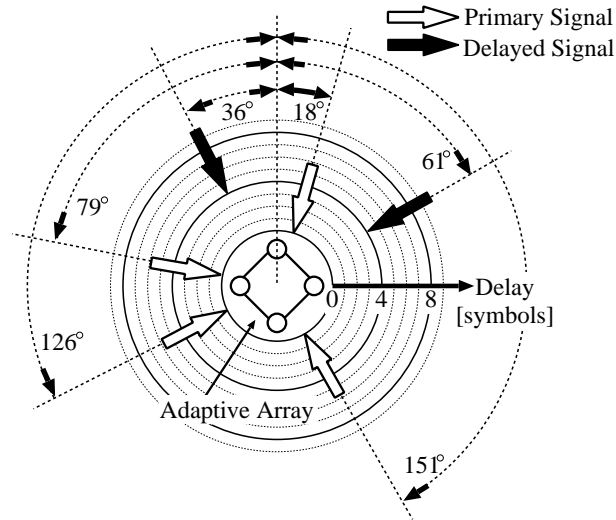


Fig. 6. Channel Model A (frequency selective fading channel)

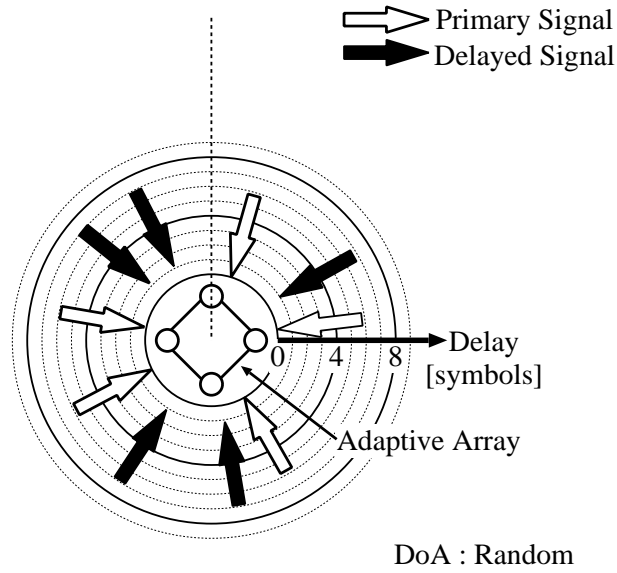


Fig. 7. Channel Model B (frequency selective fading channel)

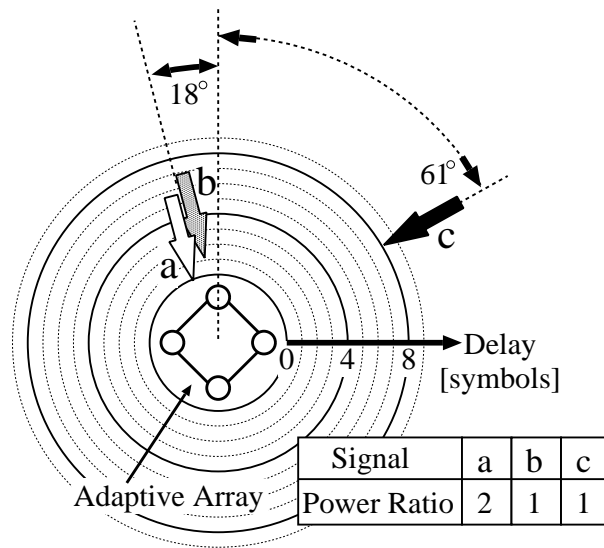


Fig. 8. Channel Model C (static 3-ray multipath channel)

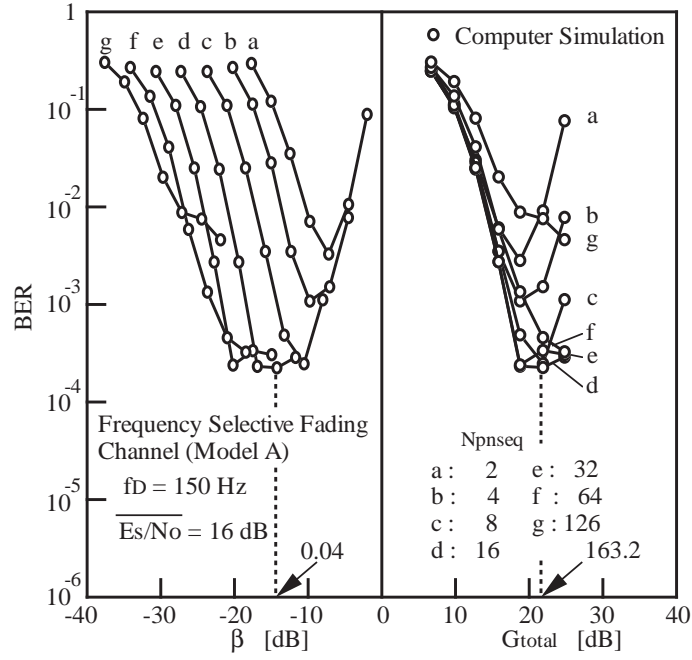


Fig. 9. Bit Error Rate versus β and G_{total}

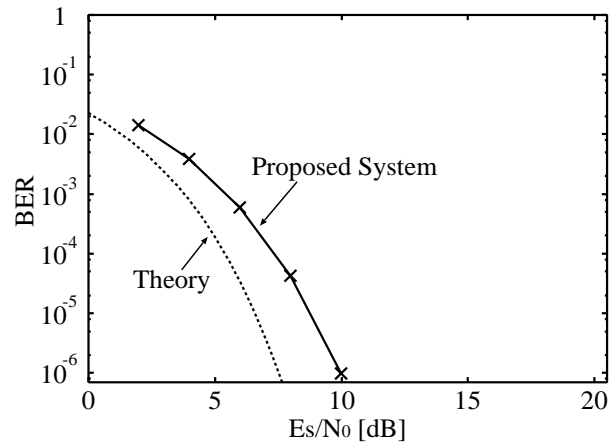


Fig. 10. Bit Error Rate Performance in AWGN Channel

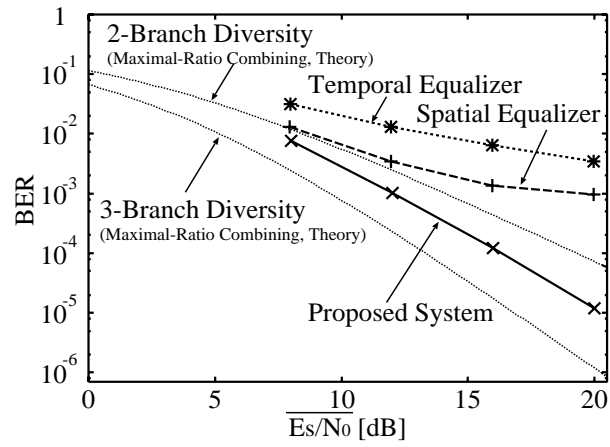


Fig. 11. Bit Error Rate Performance in Channel Model B

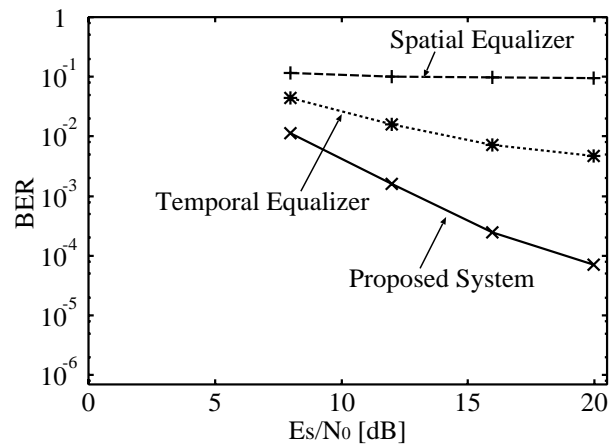


Fig. 12. Bit Error Rate Performance in Channel Model C

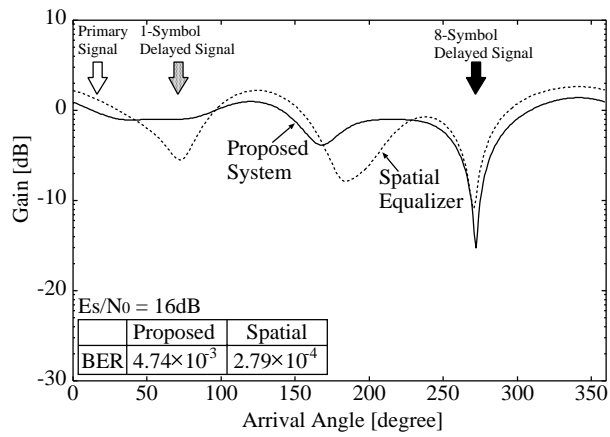


Fig. 13. Antenna Pattern a

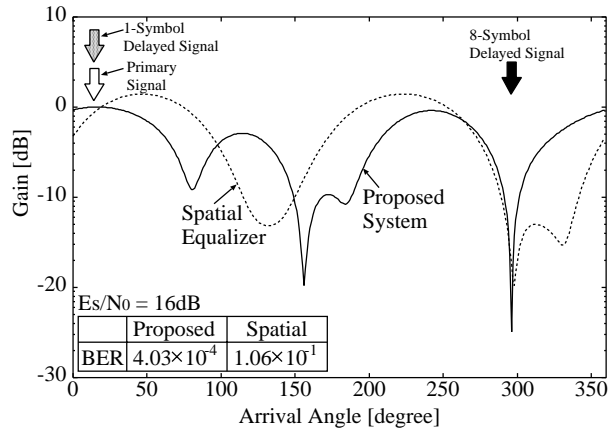


Fig. 14. Antenna Pattern b

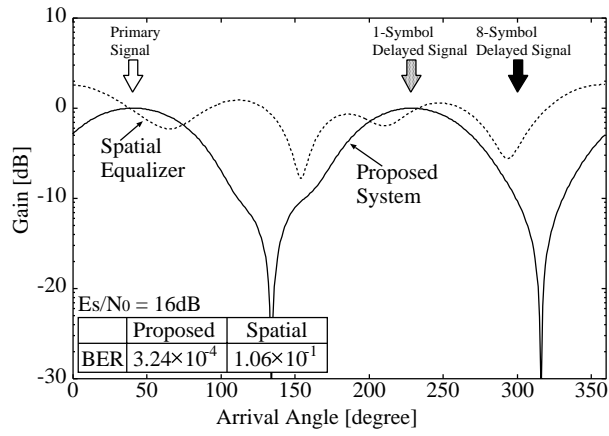


Fig. 15. Antenna Pattern c

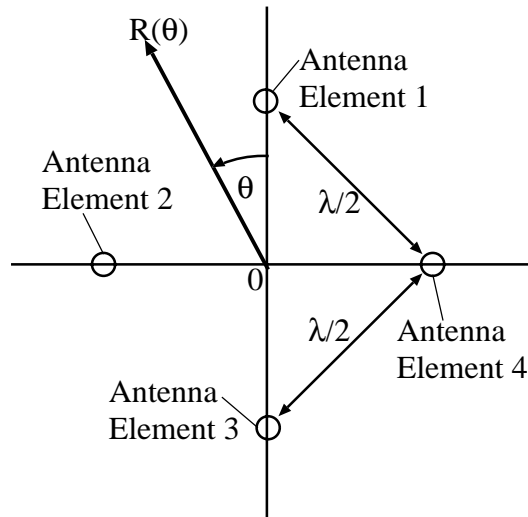


Fig. 16. Antenna Arrangement